Received: 30 September 2024 | Revised: 31 December 2024 | Accepted: 19 May 2025 | Published online: 9 June 2025

RESEARCH ARTICLE

Journal of Optics and Photonics Research
2026, Vol. 3(2) 158–165
DOI: 10.47852/bonviewJOPR52024465

BON VIEW PUBLISHING

Cost-Effective Assessment of Water Content in Indian Almond (Catappa) of Various Colored Leaves Using Continuous-Wave Terahertz Spectroscopy and Principal Component Analysis

Nagaraju Menchu[1] and Anil Kumar Chaudhary[1,*]

[1]*DRDO Industry Academia – Centre of Excellence, School of Physics, University of Hyderabad, India*

Abstract: This study presents a novel, cost-effective system using a 0.11 terahertz source and microbolometer to precisely measure water concentration in Indian almond (Catappa) leaves of various colors. We developed this system to provide accurate, nondestructive analysis of leaf water content. The system's effectiveness was validated against gravimetric analysis, confirming its reliability. Our findings revealed that the water content in Indian almond leaves follows an exponential decay pattern over time, with a high correlation ($R^2 = 0.99$). The system successfully differentiated between green and red Indian almond leaves, indicating distinct water concentrations. Additionally, measurements with the 0.11 terahertz source showed different initial values and consistent decay trends during dehydration, supporting the proportionality of absorption coefficients to water content. To enhance our analysis, we applied principal component analysis to the collected data, revealing that the first principal component accounted for approximately 94.13% of the variance, effectively summarizing the differences in water content among the leaf types. These results underscore the potential of continuous-wave terahertz spectroscopy for accurately assessing water content in Indian almond leaves of various colors, offering valuable applications in agriculture and environmental research.

Keywords: microbolometer, terahertz spectroscopy, water content, leaf, principal component analysis (PCA)

1. Introduction

Water plays a crucial role in the life cycle of plants and biomolecules, especially in leaves involved in photosynthesis and respiration. It acts as a solvent, absorbing nutrients and transporting them from the soil to plant tissues. Plants can't maintain proper turgor pressure without water, leading to wilting and impacting their morphology and color. Water scarcity further affects plant health, causing stunted growth, reduced productivity, and even death. Therefore, water availability is vital for plants' survival and proper functioning. Understanding water content in plant leaves is essential for assessing their health and growth potential. The green-colored leaf contains water, chlorophyll molecules, and other secondary metabolites responsible for photosynthesis and crop yield [1]. The water content in leaves influences their color, particularly concerning the proportion of chlorophyll and other pigments present. These pigment concentrations significantly impact the vibrant colors of autumn leaves, as chlorophyll production decreases during shorter autumn days, giving rise to robust anthocyanin and carotenoid pigments like rhodophyll, carotene, and xanthophyll, resulting in the well-known red, orange, and yellow colors of fall. Typically, leaf color variations occur before leaves fall from the tree [2–4].

Due to lower energy and greater penetration depth, terahertz (THz) radiation can be a non-invasive and nondestructive tool for analyzing explosives, drugs, and biomolecules. THz radiation is known to interact strongly with water molecules due to the high dipole moment of water. This interaction leads to a significant change in the THz radiation properties when in contact with water molecules. As a result, THz radiation is commonly utilized as a tool to measure the water content of various materials, including biological samples and polymers. Monitoring the water content in leaves is an effective means of assessing a plant's health and can provide valuable information on irrigation needs and overall physiological conditions [5]. The early detection of drought stress can help to take proactive action related to plants' health monitoring to improve overall productivity [6, 7]. Many groups, including our group, have reported the THz-based estimation of water content in different types of plant leaves and rose petals [8, 9]. The leaf's water concentration can be ascertained using THz radiation in transmission mode.

Afsah-Hejri et al. [9] have published exhaustive reports on the use of THz radiation in agricultural applications. They have emphasized the role of water contents on the drought stress of plant leaves. This has potential applications in irrigation planning and management in tropical countries like India. They have developed a qualitative model of leaf water contents that can be used to classify wet and dry leaves. Similarly, Zhang et al. [10] have introduced THz-based imaging data for calculating water contents in spinach leaves. They have developed an algorithm for

*Corresponding author: Anil Kumar Chaudhary, DRDO Industry Academia – Centre of Excellence, School of Physics, University of Hyderabad, India. Email: akcsp@uohyd.ac.in

the same. In addition, the water contents of coffee leaves were ascertained based on permittivity and reported by Jördens et al. [11]. The study conducted by Afsharinejad et al. [12] demonstrated that THz transmission could accurately measure the thickness and permittivity of coffee leaves at 130 GHz. The study's results indicated that the permittivity values were consistent across different points on the leaves, while the thickness measurements showed variations at different points. A previous report by Nie et al. [13] discussed chemometric methods to quantify water content in rapeseed leaves using THz transmission techniques. In continuation of this work, Afsharinejad et al. [14] studied the transmission loss in different types of leaves like cabbage, coffee, lettuce, mint, radish, etc., between 0.3 and 0.4 THz range. Water within the plant absorbs visible, Infrared (IR), and THz wavelengths distinctly from other structural components. Sun et al. [15] assessed the plant water status in wheat. It is important to note that water deficit is a main limiting factor in seed production. The water content in wheat leaves significantly impacts the crop's growing time, with optimal water content falling between 40 and 80%. Typically, the water content of a leaf is measured in the lab using gravimetric techniques or through fluorescence, such as delayed chlorophyll fluorescence [16]. However, these destructive methods may not provide real-time or non-invasive measurements. Finding new and innovative ways to measure water content in plant leaves without causing damage to the plant is crucial to further understanding the effects of water on plant growth and optimizing crop production.

Principal component analysis (PCA) is a powerful statistical technique that facilitates the analysis of complex datasets, such as those obtained from THz measurements. By reducing the dimensionality of the data, PCA enables the identification of key patterns and relationships between variables, enhancing the interpretation of water content variations among different leaf types. In this study, PCA was employed to analyze the beam profiles of transmitted THz radiation, allowing for effective differentiation of water content in green and red Indian almond leaves based on their spectral signatures [17, 18].

From the literature, we have identified a need for more precise and accessible methods to measure leaf water content, particularly in relation to leaf color. To address this gap, we developed a user-friendly and cost-effective setup using a continuous wave (CW) 0.11 THz source and a microbolometer. This setup, grounded in previous research findings, allows for accurate water content measurement in green and red-colored leaves from the Indian almond tree. Its portability makes it an ideal tool for field studies, enabling convenient analysis of leaf properties in diverse locations. By comparing the water content of various colored leaves with that of a dried leaf used as a reference, this setup contributes to a clearer understanding of the relationship between leaf color and water content.

2. Experimental Details

2.1. Monitoring of water status in leaves using a CW-THz source and a microbolometer camera

In this experiment, the water content of leaves was measured using THz radiation. The key components of the experimental setup include a microbolometer and an IMPATT (Impact Avalanche Transit Time) diode-based THz source, operating at 0.11 THz.

A microbolometer, also called an uncooled microbolometer, which can operate at room temperature without a cooling system, is an electronic sensor that detects electromagnetic radiation by measuring the temperature rise in a sensitive material. In this setup, the microbolometer was used for beam profiling, detecting the intensity distribution of THz radiation. When the microbolometer is exposed to CW-THz radiation, it experiences a temperature rise, which is detected by monitoring changes in its electrical resistance. The two-dimensional beam profile was obtained by scanning the microbolometer across the beam.

The IMPATT diode used in this experiment serves as the THz radiation source. These diodes generate THz radiation by exploiting avalanche breakdown in the semiconductor material. When the diode is biased with a direct current (DC) voltage, high-frequency oscillations are generated, which are then used to power an antenna to emit THz radiation. IMPATT diodes are known for their compact size, high power output, and wide tunability, making them ideal for THz imaging, sensing, and spectroscopy applications [19–21].

2.1.1. Experimental setup

The experimental system consists of a commercially available THz camera from neTHIS (Model: OpenVIEW) and a 0.11 THz IMPATT diode-based THz source from Terasense. A special Tsurupica aspheric lens with a 3 cm focal length was used to focus the THz radiation onto the camera. To achieve precise focusing and minimize aberrations, an aperture was placed in front of the THz source to eliminate highly diverging rays, resulting in a tightly focused beam with a 5 mm diameter. The leaf samples were placed between the lens and the camera to measure the interaction of THz radiation with the leaf material. A schematic of the experimental setup is shown in Figure 1(a).

Figure 1

(a) Schematic of the experimental setup for leaf's water content measurement and (b) photographic images of two different colored Indian almond leaves used to study the water content measurements

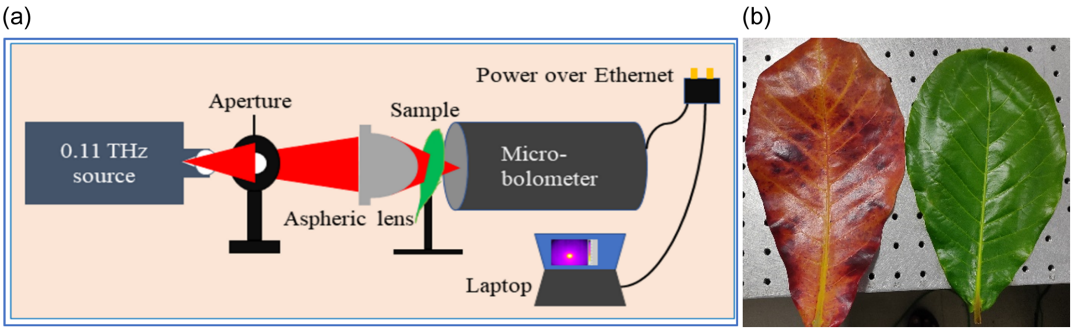

Table 1
Details of the microbolometer camera Model: OpenViewTHz-320

Specification	Details
Type	Real-time
Camera model and serial no	FLIR AX5 and 26422
Spectral band	0.1 – 30 *THz*
Sensitive detection area	54.4 × 43.5 mm^2
Pixel numbers	320 × 256 pixels
Spatial resolution	170 μm
Frequency rate	30 *Hz*/60 *Hz*
Minimum measurable signal	50 $\mu W/cm^2$
Damage threshold	1 W/cm^2
Vision and acquisition software	ResearchIR

The IMPATT diode operates in CW mode at 0.11 THz and is employed to generate THz radiation. The radiation is directed toward the leaf samples through the aspheric lens, ensuring precise beam profiling. Data acquisition is performed using proprietary ResearchIR software, which enables the measurement of the intensity distribution and temperature of the radiation, allowing for detailed analysis of the leaf's interaction with the THz radiation. With the carefully positioned components, the setup's design ensures high-quality measurements with minimal interference, allowing for accurate characterization of the water content in the leaves.

Further, the microbolometer camera and THz source details are provided in Tables 1 and 2, respectively.

Table 2
Details of the terahertz source

Specification	Details
Wavelength	110 *GHz*
Average power	60 *mW*
Conical horn	Yes
TTL Modulation	Yes

2.1.2. Leaf sample preparation

Two types of leaves, green and red, were plucked from the Indian almond tree. The leaves were cleaned using dry tissue to remove any dirt or contaminants. The outline of each leaf was drawn on paper to measure the leaf area, and a known scale was used to enable measurements with the FIJI software. The leaf thickness was also measured at multiple points using a vernier caliper, and the average thickness was recorded to calculate the absorption coefficient. The leaf weights were also recorded to determine the water content, which was measured manually by subtracting the weight of the fully dried leaf from the wet leaf weight. This process was repeated at different drying stages to observe the dehydration mechanism of the leaf samples. The leaf samples used in this experiment are shown in Figure 1(b).

2.1.3. Experimental procedure and data collection

The microbolometer camera was initially calibrated by removing background noise from ambient room temperature using the ResearchIR software and setting the system to approximately 0 K. The THz beam profile was first captured without leaf samples. Using the software, average intensity (in counts) and temperature (in Kelvin) were measured by defining a circular region of interest around the beam spot. These reference beam profiles are shown in Figure 2(a). Samples were positioned between the aspheric lens and the camera for the leaf experiments. The captured beam profiles of

Figure 2
The beam profiles of the 0.11 THz source captured using an uncooled microbolometer: (a) direct beam, (b) transmitted through the green leaf, and (c) transmitted through the red leaf

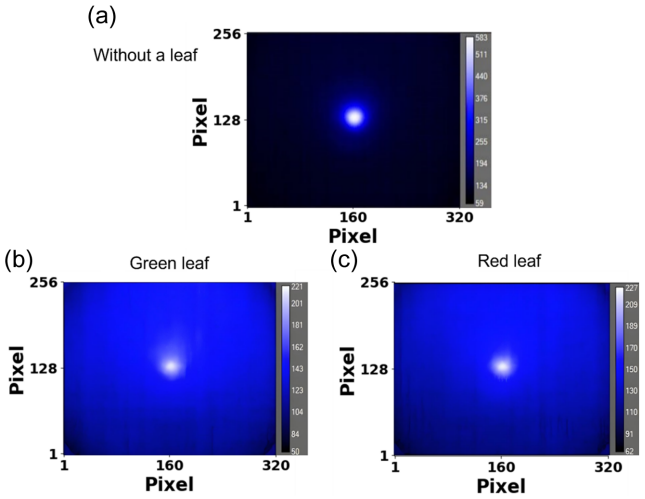

the green and red leaves are shown in Figure 2(b) and (c), respectively. The procedure was repeated for each leaf at various drying stages to analyze the effect of water content on the THz beam transmission. After 93 h of natural dehydration, the leaves were oven-dried for 40 min at 70 °C to ensure complete dehydration. The captured data, including intensity and temperature values, were summarized in Tables 3 and 4. Throughout the experiment, the thickness and weight of the leaf samples were measured at each drying stage. Leaf thickness was determined by averaging multiple measurements taken with a vernier caliper (precision: 0.05 mm), and the weight was assessed using a microbalance (precision: 0.01 mg). These measurements enabled an evaluation of changes in the leaf's physical properties, such as thickness and water weight, as it dehydrated. This detailed assessment, along with the corresponding THz measurements, is presented in tabular format in Tables 3 and 4.

3. Results and Discussions

3.1. THz and gravimetry analysis

Figure 2 shows the beam profiles of THz radiation captured using a microbolometer. When no sample was placed between the source and camera, the beam profile was circular, and no scattering was observed around the spot, as shown in Figure 2(a). The spot was also brighter and had a higher average intensity in counts, indicating the absence of any interaction between the radiation and the sample. The average counts were measured using a circle wrapped around the illuminated area, and the results showed a high value for the spot without any sample. This finding confirms that the circular shape of the beam profile and the high average counts are due to the absence of any sample that could cause scattering of the beam. The beam profiles of the green and red color almond leaves are shown in Figure 2(b) and (c), respectively. The results showed that the green leaf had the lowest average counts, and the beam scattered more around the circular spot than the red leaf. This can be attributed to the higher water content in the green leaf, which causes more beam scattering due to the THz radiation's interaction with the leaf's water molecules.

Table 3
The initial red leaf area, weight, and average thickness at varying dehydration times, along with the intensity and temperature of the measured terahertz beam at 0.11 THz frequency using a microbolometer, were recorded at the same time

				Without leaf		With red leaf	
Area of the red leaf (cm^2)	Time (*Hrs*).	Weight of the leaf (g)	Avg. thickness (mm)	Avg. Counts ($a.u$)	Avg. Temp (K)	Avg. Counts ($a.u$)	Avg. Temp (K)
290	0	4.636	0.12	375	4.4	163	2
	19	2.926	0.08	567	7.5	483	6.6
	43	2.724	0.07	435	5.2	410	4.9
	72	2.611	0.065	485	6.5	464	6.4
	93	2.457	0.057	600	8.6	595	8.6

Table 4
The initial green leaf area, weight, and average thickness at varying dehydration times, along with the intensity and temperature of the measured terahertz beam at 0.11 THz frequency using a microbolometer, were recorded at the same time

				without leaf		with green leaf	
Area of the green leaf (cm^2)	Time (h)	Weight of the leaf (g)	Avg. thickness (mm)	Avg. Counts ($a.u$)	Avg. Temp (K)	Avg. Counts ($a.u$)	Avg. Temp (K)
226	0	5.33	0.13	374	4.35	119	1.47
	19	2.79	0.075	567	7.7	516	7.3
	43	2.396	0.072	435	5.3	420	5.14
	72	2.239	0.065	430	5.85	420	5.8
	93	2.077	0.05	530	8	525	7.9

In contrast, the red leaf had lower water content, resulting in less beam scattering and higher average counts. The beam profile is an important factor in THz spectroscopy, and the observed differences between green and red leaves indicate the potential of THz radiation for non-invasive analysis of plant water content. The beam profiles and average counts obtained in this study can serve as a valuable reference for future research employing THz radiation in a wide range of applications, such as material analysis and biomedical imaging, as well as for investigations related to plant physiology, agriculture, and the advancement of THz spectroscopy techniques for plant analysis.

Based on obtained experimental data, various stages of water status parameters were calculated using the following formulas:

The water concentration of the leaf was calculated using the below formula:

$$C(\%) = \frac{W_t(g) - W_{dry}(g)}{W_t(g)} \quad (1)$$

"Wt" is the weight of the leaf sample (in *grams*) measured at a particular time point during the experiment, while "Wdry" is the weight of the sample when it was fully dried in an oven at 100 °C for one hour at the end of the experiment.

The water mass per unit area was calculated using the following formula:

$$WMA\left(\frac{g}{cm^2}\right) = \left(\frac{W_t(g) - W_{dry}(g)}{Area\ of\ the\ leaf\ in\ cm^2}\right) \quad (2)$$

The absorption coefficients of the leaves were calculated using the Beer-Lambert law. This law relates the absorption of light by a material to the material's thickness, concentration, and wavelength of the light. By measuring the intensity of the THz beam transmitted through the leaves and using the thickness measurements obtained earlier, the absorption coefficient of the leaves was calculated.

$$Absorption\ coefficient\ (cm^{-1}) = -\frac{1}{d} Ln\left(\frac{I}{I_0}\right) \quad (3)$$

where d is the average thickness of the leaf (in *centimeters*), I is the average intensity (in terms of *counts*) of the THz beam transmitted through the leaf sample, I_0 is the beam's intensity without the leaf sample.

The percent change in temperature (temperature measured in Kelvins) was calculated using the following formula.

$$\%\ Change\ in\ temperature = \frac{T_{ws}(K) - T_{leaf}(K)}{T_{ws}(K)}\ X\ 100 \quad (4)$$

where $T_{ws}(K)$ is the temperature of the beam without the leaf and $T_{leaf}\ (K)$ is the temperature of the beam after passing through the leaf.

Table 5 provides a comprehensive overview of all the calculated parameters for both green and red leaves, including their respective units of measurement.

The data obtained from the study were plotted into graphs, as shown in Figure 3, by comparing the water content in both green and red leaves. The data were then fitted to an exponential decay curve, and the data fitting was successful with all fits above the 0.99 fitting parameters. This suggests that the water in the Indian almond leaves follows a decay process while dehydrating. Both gravimetric and THz data showed a similar trend and followed exponential decay [22–25]. The calculated data is shown in symbols in the graph, while the fitted data is in solid lines. Figure 3 shows the variation of different water status parameters while dehydrating the green and red leaves. It is evident from these graphs that the green leaf has a higher water concentration, and the water mass per unit area is also higher than the red leaf [26]. These calculations were done using gravimetry analysis, as shown in Figure 3(a) and (b). In Figure 3(c) and (d), the THz results are shown, which also clearly demonstrate that the green leaf has a higher water concentration by observing the absorption coefficient and percentage change in the transmitted temperature

Table 5
The calculations of different water status parameters measured using gravimetric analysis and microbolometer-based terahertz transmission setup

	Green leaf				Red leaf			
Time (*h*)	Water Conc. (%)	% Change in temp.	WMA (g/cm^2) * 10^{-3}	Abs. Coeff (cm^{-1})	Water Conc. (%)	WMA (g/cm^2) * 10^{-3}	% Change in temp.	Abs. Coeff (cm^{-1})
0	61.03	66.1	14.39	86.4	47	7.51	54.5	69.4
19	13.42	5.2	3.16	12.6	10.1	1.62	12	20.7
43	5.99	3.2	1.41	4.8	5.7	0.92	5.78	8.4
72	3.05	0.8	0.8	3.62	3.31	0.53	1.54	6.81
93	0	0.5	0	1.9	0	0	0	1.45

Figure 3
The variation in (a) the water concentration (%), (b) water mass per unit area, (c) absorption coefficient, and (d) % change in temperature with respect to time

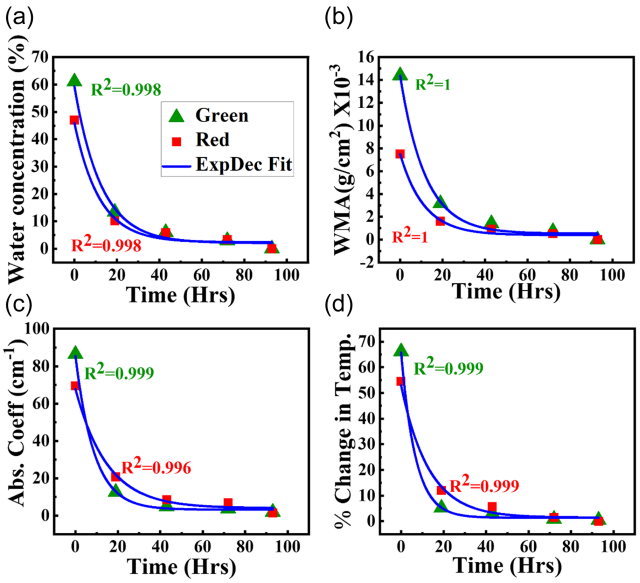

Note: The experiment was performed using a 0.11 THz source and microbolometer camera. The data are fitted to the exponential decay function, and the fitting parameter is shown separately for different leaves data.

of the beam. The results from both experiments match successfully. Figure 4 shows the water status parameters measured using both gravimetry and the THz setup. The linear relationship between these measurements indicates that the THz-based assessment of leaf water content is accurate and reliable. Specifically, the absorption coefficient, measured through THz transmission, correlates linearly with the water concentration determined by the gravimetry method. This linear trend confirms the efficacy and potential of using THz technology for precise leaf water content measurement.

Overall, the obtained data plotted into graphs by comparing the water content in green and colored leaves yielded important insights into the water content of leaves during the dehydration process. The data were fit to an exponential decay curve, and the data fitting was successful, with all fits above the 0.99 fitting parameters. The results from gravimetry and THz data analysis showed similar trends, with both data types following exponential decay. These findings suggest that the water content in leaves follows a decay process while

Figure 4
The variation in (a) the % change in temperature and (b) the absorption coefficient of green and red leaves with respect to water concentration

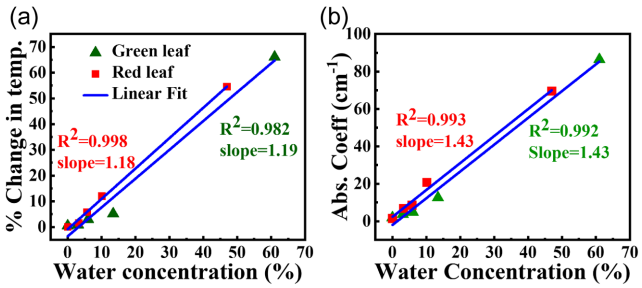

dehydrating. As the gravimetry and THz results demonstrate, green leaves' high water concentration and water mass per unit area have significant implications for understanding plant physiology and future research.

3.2. PCA approach to analyzing leaf water content measurements

In this analysis, we apply PCA technique to differentiate between three categories of leaf profiles—green leaf, red leaf, and without leaf—using intensity profiles of transmitted THz radiation captured by a bolometer. This approach allows us to effectively explore the water content variance among these leaf types.

3.2.1. Data preparation

The dataset consists of intensity values measured at a frequency of 0.11 THz, recorded for three leaf categories. Each leaf category is represented by a set of pixel intensity values derived from images. The intensity values are organized as follows:

1) **Green leaf:** Intensity profile for green leaves.
2) **Red leaf:** Intensity profile for red leaves.
3) **Without leaf:** Intensity profile for leaves without any foliage.

3.2.2. Understanding PCA

PCA is a statistical method used to reduce the dimensionality of data while preserving as much variance as possible. It transforms the original variables (in this case, pixel intensity values) into a new set of variables called principal components (PCs). The first principal component (PC1) captures the most variance, while the second principal component (PC2) captures the second most variance [27–33].

3.2.3. Mathematical steps in PCA

1) Standardization

Before applying PCA, the data are standardized to have a mean of 0 and a standard deviation of 1. This ensures that all intensity values contribute equally to the analysis. For each intensity value $I_{n,i}$ (where n is the pixel position and i is the image index):

$$Z_{n,i} = \frac{(I_{n,i} - \mu_n)}{\sigma_n} \tag{5}$$

Where:

1) μ_n is the mean intensity for pixel n across all images.
2) σ_n is the standard deviation for pixel n.

2) Covariance matrix

The covariance matrix C is computed to understand how the pixel intensities vary together:

$$C = \frac{1}{(m-1)} Z^T Z \tag{6}$$

Z is the matrix of standardized pixel values and m is the number of images.

3) Eigenvalues and eigenvectors

The eigenvalues and eigenvectors of the covariance matrix are calculated. The eigenvalues indicate the amount of variance captured by each PC, while the eigenvectors represent the directions of these components.

4) PCs

The PCs are obtained by projecting the standardized data onto the eigenvectors:

$$PC = Z \cdot V \tag{7}$$

The projection of the i-th image onto the PC1:

$$PC1_i = Z_i \cdot V_1 \tag{8}$$

The projection of the i-th image onto the PC2:

$$PC2_i = Z_i \cdot V_2 \tag{9}$$

where V is the matrix of eigenvectors, each image is thus represented by a single point in the PCA space defined by its projections onto the first two PCs (PC1 and PC2).

3.2.4. PCA results and explained variance

The PCA results shown in Figure 5 reveal significant insights into the variance captured by the PCs:

1) PC1: 0.94129763 (approximately 94.13%)
2) PC2: 0.05870237 (approximately 5.87%)

These results indicate that PC1 accounts for a substantial majority of the variance in the dataset, effectively summarizing the differences in water content among the leaf types. The high explained variance by PC1 suggests that it is primarily influenced by the water content in the leaves.

Figure 5
PCA of terahertz beam profile images of the different colored leaves

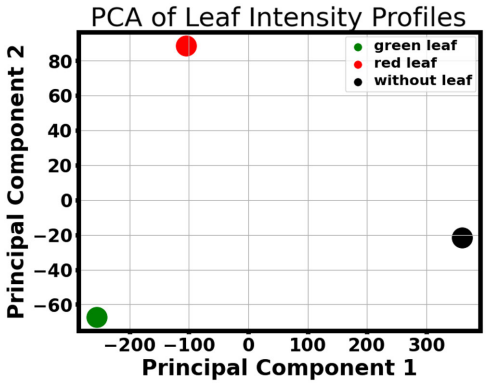

3.2.5. PC values for leaf categories

The PC values for the different leaf categories are summarized as follows:

1) Green leaf: PC1 = −255.05, PC2 = −67.15
2) Red leaf: PC1 = −105.35, PC2 = 88.73
3) Without leaf: PC1 = 360.39, PC2 = −21.58

These values indicate that:

1) Green leaf: Have the most negative PC1 values, suggesting a lower intensity profile due to higher water content.
2) Red leaf: Exhibit less negative PC1 values, indicating lower water concentrations.
3) Without leaf: Shows a positive PC1 value, highlighting a distinct profile that differs significantly from the leaves.

3.2.6. Implications of PCA in water content analysis

The PCA technique effectively differentiates the water content in Indian almond leaves, providing a robust method for analyzing THz radiation intensity profiles. The significant variance captured by PC1 allows for effectively classifying leaf types based on their water content. It addresses limitations associated with traditional ROI measurements, where scattering beams may not be perfectly circular for leaves with higher water content. This study demonstrates that PCA can enhance the understanding of leaf water content differences, making it a valuable tool in botanical research and THz imaging applications.

4. Conclusions

We successfully developed a simple, portable, and cost-effective system utilizing a 0.11 THz source and a microbolometer for accurate measurement of water concentration in leaves. Our key finding is that this system effectively distinguishes between green and red leaves, revealing distinct water concentrations and highlighting its high sensitivity. The gravimetric analysis demonstrated that the water content with respect to dehydration time follows an exponential decay pattern with a high correlation ($R^2 = 0.99$). Additionally, the absorption and percentage temperature change measured using the 0.11 THz source showed different values at the initial time, indicating varying water concentrations between leaf types. Both leaf types exhibited the same decay trend during dehydration, suggesting that the absorption coefficient is proportional to water content.

Importantly, the linear trend observed between the gravimetric and THz results confirms the reliability of THz spectroscopy for assessing leaf water content. These results underscore the potential of continuous-wave THz spectroscopy as a powerful diagnostic tool for monitoring water content in both green and colored leaves, offering valuable applications in agriculture and environmental research. This technology enables more precise and nondestructive plant health and hydration, paving the way for improved crop management strategies.

Furthermore, the application of PCA to the intensity profiles of transmitted THz radiation allowed for effective differentiation of leaf types based on their water content. The PCA results indicated that the first PC captured the majority of the variance (PC1 = 94.13%), providing valuable insights into the relationships between the different categories of hydration assessment.

Recommendations

Integrate THz Technology: Integrate the 0.11 THz spectroscopy system into agricultural practices for precise, nondestructive monitoring of leaf water content. **Expand Research:** Conduct further studies on various plant species with differently colored leaves to examine their water content and physiological relationships. **Establish Monitoring Protocols:** Develop standardized protocols for routine assessment of leaf water content to optimize irrigation practices and improve drought management strategies.

Funding Support

This work is sponsored by the Defence Research and Development Organisation, DIA-CoE (ACRHEM) under Phase III (project No. ERIP/ER/1501138/M/01/319/D (R&D)).

Ethical Statement

This study does not contain any studies with human or animal subjects performed by any of the authors.

Conflicts of Interest

The authors declare that they have no conflicts of interest to this work.

Data Availability Statement

Data are available from the corresponding author upon reasonable request.

Author Contribution Statement

Nagaraju Menchu: Conceptualization, Methodology, Software, Validation, Formal analysis, Investigation, Resources, Data curation, Writing – original draft, Writing – review & editing, Visualization. **Anil Kumar Chaudhary:** Conceptualization, Methodology, Software, Validation, Investigation, Resources, Data curation, Writing – review & editing, Supervision, Project administration, Funding acquisition.

References

[1] Zhang, Y., Wang, X., Wang, Y., Hu, L., & Wang, P. (2023). Detection of tomato water stress based on terahertz spectroscopy. *Frontiers in Plant Science*, *14*, 1095434. https://doi.org/10.3389/fpls.2023.1095434

[2] Liu, Y., Feng, X., Zhang, Y., Zhou, F., & Zhu, P. (2021). Simultaneous changes in anthocyanin, chlorophyll, and carotenoid contents produce green variegation in pink-leaved ornamental kale. *BMC Genomics*, *22*(1), 455. https://doi.org/10.1186/s12864-021-07785-x

[3] Ye, Y., & Zhang, X. (2021). Exploration of global spatiotemporal changes of fall foliage coloration in deciduous forests and shrubs using the VIIRS land surface phenology product. *Science of Remote Sensing*, *4*, 100030. https://doi.org/10.1016/j.srs.2021.100030

[4] Paudel, A., Brown, J., Upadhyaya, P., Asad, A. B., Kshetri, S., Davidson, J. R., . . . , & Karkee, M. (2024). *Machine vision-based assessment of fall color changes and its relationship with leaf nitrogen concentration*. arXiv. https://doi.org/10.48550/arXiv.2404.14653

[5] Li, B., & Zhao, X. (2018). Monitoring soybean leaf water status using terahertz spectroscopy. In *2018 43rd International Conference on Infrared, Millimeter, and Terahertz Waves*, 1. https://doi.org/10.1109/IRMMW-THz.2018.8510251

[6] Li, B., Long, Y., & Yang, H. (2018). Measurements and analysis of water content in winter wheat leaf based on terahertz spectroscopy. *International Journal of Agricultural and Biological Engineering*, *11*(3), 178–182. https://doi.org/10.25165/j.ijabe.20181103.3520

[7] López-López, M., Calderón, R., González-Dugo, V., Zarco-Tejada, P. J., & Fereres, E. (2016). Early detection and quantification of almond red leaf blotch using high-resolution hyperspectral and thermal imagery. *Remote Sensing*, *8*(4), 276. https://doi.org/10.3390/rs8040276

[8] Damarla, G., Chaudhary, A. K., & Venkatesh, M. (2017). Study of water loss in the rose petals using terahertz spectroscopy. In *2017 IEEE Workshop on Recent Advances in Photonics*, 1–3. https://doi.org/10.1109/WRAP.2017.8468575

[9] Afsah-Hejri, L., Akbari, E., Toudeshki, A., Homayouni, T., Alizadeh, A., & Ehsani, R. (2020). Terahertz spectroscopy and imaging: A review on agricultural applications. *Computers and Electronics in Agriculture*, *177*, 105628. https://doi.org/10.1016/j.compag.2020.105628

[10] Zhang, H., Mitobe, K., & Yoshimura, N. (2008). Terahertz imaging for water content measurement. In *2008 International Symposium on Electrical Insulating Materials*, 87–90. https://doi.org/10.1109/ISEIM.2008.4664503

[11] Jördens, C., Scheller, M., Breitenstein, B., Selmar, D., & Koch, M. (2009). Evaluation of leaf water status by means of permittivity at terahertz frequencies. *Journal of Biological Physics*, *35*(3), 255–264. https://doi.org/10.1007/s10867-009-9161-0

[12] Afsharinejad, A., Davy, A., O'Leary, P., & Brennan, C. (2017). Transmission through single and multiple layers of plant leaves at THz frequencies. In *2017 IEEE Global Communications Conference*, 1–6. https://doi.org/10.1109/GLOCOM.2017.8254561

[13] Nie, P., Qu, F., Lin, L., Dong, T., He, Y., Shao, Y., & Zhang, Y. (2017). Detection of water content in rapeseed leaves using terahertz spectroscopy. *Sensors*, *17*(12), 2830. https://doi.org/10.3390/s17122830

[14] Afsharinejad, A., Davy, A., & Naftaly, M. (2017). Variability of terahertz transmission measured in live plant leaves. *IEEE Geoscience and Remote Sensing Letters*, *14*(5), 636–638. https://doi.org/10.1109/LGRS.2017.2667225

[15] Sun, H., Feng, M., Xiao, L., Yang, W., Wang, C., Jia, X., . . . , & Li, D. (2019). Assessment of plant water status in winter wheat (*Triticum aestivum* L.) based on canopy spectral

indices. *PLoS One*, *14*(6), e0216890. https://doi.org/10.1371/journal.pone.0216890

[16] Borovkova, M., Khodzitsky, M., Demchenko, P., Cherkasova, O., Popov, A., & Meglinski, I. (2018). Terahertz time-domain spectroscopy for non-invasive assessment of water content in biological samples. *Biomedical Optics Express*, *9*(5), 2266–2276. https://doi.org/10.1364/boe.9.002266

[17] Füzy, A., Kovács, R., Cseresnyés, I., Parádi, I., Szili-Kovács, T., Kelemen, B., …, & Takács, T. (2019). Selection of plant physiological parameters to detect stress effects in pot experiments using principal component analysis. *Acta Physiologiae Plantarum*, *41*(5), 56. https://doi.org/10.1007/s11738-019-2842-9

[18] Oda, N., Kurashina, S., Miyoshi, M., Doi, K., Ishi, T., Sudou, T., …, & Sasaki, T. (2015). Microbolometer terahertz focal plane array and camera with improved sensitivity in the sub-terahertz region. *Journal of Infrared, Millimeter, and Terahertz Waves*, *36*(10), 947–960. https://doi.org/10.1007/S10762-015-0184-2

[19] Tzydynzhapov, G., Gusikhin, P., Muravev, V., Dremin, A., Nefyodov, Y., & Kukushkin, I. (2020). New real-time sub-terahertz security body scanner. *Journal of Infrared, Millimeter, and Terahertz Waves*, *41*(6), 632–641. https://doi.org/10.1007/s10762-020-00683-5

[20] Zhang, H., Sfarra, S., Saluja, K., Peeters, J., Fleuret, J., Duan, Y., …, & Maldague, X. (2017). Nondestructive investigation of paintings on canvas by continuous wave terahertz imaging and flash thermography. *Journal of Nondestructive Evaluation*, *36*(2), 34. https://doi.org/10.1007/S10921-017-0414-8

[21] Li, R., Lu, Y., Peters, J. M. R., Choat, B., & Lee, A. J. (2020). Non-invasive measurement of leaf water content and pressure–volume curves using terahertz radiation. *Scientific Reports*, *10*(1), 21028. https://doi.org/10.1038/s41598-020-78154-z

[22] Li, B., Zhang, X., Wang, R., Mei, Y., & Ma, J. (2021). Leaf water status monitoring by scattering effects at terahertz frequencies. *Spectrochimica Acta Part A: Molecular and Biomolecular Spectroscopy*, *245,* 118932. https://doi.org/10.1016/j.saa.2020.118932

[23] Federici, J. F. (2012). Review of moisture and liquid detection and mapping using terahertz imaging. *Journal of Infrared, Millimeter, and Terahertz Waves*, *33*(2), 97–126. https://doi.org/10.1007/s10762-011-9865-7

[24] Altay, K., Hayaloglu, A. A., & Dirim, S. N. (2019). Determination of the drying kinetics and energy efficiency of purple basil (*Ocimum basilicum* L.) leaves using different drying methods. *Heat and Mass Transfer*, *55*(8), 2173–2184. https://doi.org/10.1007/s00231-019-02570-9

[25] Girolamo, F. V. D., Toncelli, A., Tredicucci, A., Bitossi, M., & Paoletti, R. (2020). Leaf water diffusion dynamics in vivo through a sub-terahertz portable imaging system. *Journal of Physics: Conference Series*, *1548*(1), 012002. https://doi.org/10.1088/1742-6596/1548/1/012002

[26] Menchu, N., Ghorui, C., Damarla, G., & Chaudhary, A. K. (2021). THz-TDS as a diagnostic tool for monitoring the water content in different coloured Indian almond leaves. In *Frontiers in Optics + Laser Science 2021*, JW7A.59. https://doi.org/10.1364/FIO.2021.JW7A.59

[27] Greenacre, M., Groenen, P. J. F., Hastie, T., D'Enza, A. I., Markos, A., & Tuzhilina, E. (2022). Principal component analysis. *Nature Reviews Methods Primers*, *2*(1), 100. https://doi.org/10.1038/s43586-022-00184-w

[28] Uddin, M. P., Mamun, M. A., & Hossain, M. A. (2021). PCA-based feature reduction for hyperspectral remote sensing image classification. *IETE Technical Review*, *38*(4), 377–396. https://doi.org/10.1080/02564602.2020.1740615

[29] Mahanti, N. K., Pandiselvam, R., Kothakota, A., Ishwarya, S. P., Chakraborty, S. K., Kumar, M., & Cozzolino, D. (2022). Emerging nondestructive imaging techniques for fruit damage detection: Image processing and analysis. *Trends in Food Science & Technology*, *120*, 418–438. https://doi.org/10.1016/j.tifs.2021.12.021

[30] Wang, C., Liu, B., Liu, L., Zhu, Y., Hou, J., Liu, P., & Li, X. (2021). A review of deep learning used in the hyperspectral image analysis for agriculture. *Artificial Intelligence Review*, *54*(7), 5205–5253. https://doi.org/10.1007/s10462-021-10018-y

[31] Dua, Y., Kumar, V., & Singh, R. S. (2020). Comprehensive review of hyperspectral image compression algorithms. *Optical Engineering*, *59*(9), 090902. https://doi.org/10.1117/1.OE.59.9.090902

[32] Park, H., & Son, J.-H. (2021). Machine learning techniques for THz imaging and time-domain spectroscopy. *Sensors*, *21*(4), 1186. https://doi.org/10.3390/s21041186

[33] Wang, C., Zhou, R., Huang, Y., Xie, L., & Ying, Y. (2019). Terahertz spectroscopic imaging with discriminant analysis for detecting foreign materials among sausages. *Food Control*, *97*, 100–104. https://doi.org/10.1016/j.foodcont.2018.10.024

How to Cite: Menchu, N., & Chaudhary, A. K. (2026). Cost-Effective Assessment of Water Content in Indian Almond (Catappa) of Various Colored Leaves Using Continuous-Wave Terahertz Spectroscopy and Principal Component Analysis. *Journal of Optics and Photonics Research*, *3*(2), 158–165. https://doi.org/10.47852/bonviewJOPR52024465